Ring, J. D., Howls, C. J., & Dennis, M. R. (2013). Incomplete Airy beams: finite energy from a sharp spectral cutoff. Optics letters, 38(10), 1639-1641. 10.1364/OL.38.001639

Incomplete Airy beams: finite energy from a sharp spectral cutoff

James D. Ring,[1,*] Christopher J. Howls,[2] and Mark R. Dennis[1]

[1]*H H Wills Physics Laboratory, University of Bristol, Tyndall Avenue, Bristol BS8 1TL, UK*

[2]*School of Mathematics, University of Southampton, Highfield, Southampton SO17 1BJ, UK*

**Corresponding author: james.ring@bristol.ac.uk*

Received February 7, 2013; revised April 12, 2013; accepted April 12, 2013;
posted April 15, 2013 (Doc. ID 185038); published May 9, 2013

We present a mathematical analysis of the finite-energy Airy beam with a sharply truncated spectrum, which can be generated by a uniformly illuminated, finite-sized spatial light modulator, or windowed cubic phase mask. The resulting "incomplete Airy beam" is tractable mathematically, and differs from an infinite-energy Airy beam by an additional oscillating modulation and the decay of its fringes. Its propagation can be described explicitly using an incomplete Airy function, from which we derive simple expressions for the beam's total power and mean position. Asymptotic analysis reveals a simple connection between the cutoff and the region of the beam with Airy-like behavior.

OCIS codes: (090.0090) Holography; (000.3860) Mathematical methods in physics; (070.2580) Paraxial wave optics.
http://dx.doi.org/10.1364/OL.38.001639

An increasing number of optical beams with remarkable properties have been studied which, in a mathematical sense at least, have infinite energies. Strictly, they have transverse intensity profiles that cannot be normalized. Bessel, Airy, and Pearcey beams [1–3] are three such examples and only approximations of these beams are realizable experimentally [3–6]. The question of how such finite-energy beams are described mathematically can be a subtle one, but often provides important physical insight into their behavior. Here we consider how it limits the region of acceleration of finite-energy Airy beams.

The most commonly considered finite-energy Airy beam, introduced in [5], uses an exponential apodization and relies on the rapid decay of the Airy function for positive arguments. Alternatively, finite-energy can be enforced by modulating the Airy function with a wide Gaussian profile [6], or even by a sharp truncation [7–9]. These beams display good approximations of the transverse acceleration of infinite-energy Airy beams over an appreciable propagation distance.

However, finiteness of energy can also be enforced by limiting the beam's spectrum [8–12], which is more practical as the simple Airy spectrum is easy to generate and manipulate [10,11] experimentally. In the laboratory, this is done by illuminating a cubic phase mask (or spatial light modulator) with a Gaussian beam [5,11], or using a finite-sized cubic element or hard aperture [8–10].

In this Letter, we present a mathematical analysis of the finite-energy Airy beam generated from a sharply truncated Airy spectrum with uniform amplitude between its limits. Such beams have been studied numerically [8–10], but our new analysis reveals a simple connection between the cutoff and the region of the beam that exhibits Airy-like behavior, as well as giving a limit for the extent of the main intensity lobe. The sharp spectral cutoff causes the beam to differ from the ideal Airy beam, having an extra oscillating modulation in addition to the desired decay of its fringes. Physically, sharp discontinuities may result in complicated analytic expressions, but in the case we present, the results are pleasingly elegant, based on the definition of an incomplete Airy function [13,14].

The infinite-energy Airy beam is obtained from paraxial propagation of the Airy function [15], which itself is defined as an integral

$$\mathrm{Ai}(X) = \frac{1}{2\pi}\int_{-\infty}^{\infty} \mathrm{d}\xi \, \exp\left[i\left(\frac{1}{3}\xi^3 + \xi X\right)\right], \tag{1}$$

where $X \equiv \kappa x$ is the dimensionless transverse distance and κ is an inverse length which governs the transverse scale of the beam. Equation (1) is interpreted as a Fourier representation, so the spectrum of $\mathrm{Ai}(X)$ is $\widehat{\mathrm{Ai}}(\xi) = \exp(i\xi^3/3)/2\pi$, with ξ the Fourier partner of X. The intensity of $\mathrm{Ai}(X)$ is shown in Fig. 1(a). The decay of the intensity fringes is proportional to $(-X)^{-1/2}$, so the integral of $|\mathrm{Ai}(X)|^2$ over all X does not converge.

The paraxial, infinite-energy Airy beam we write as $\mathrm{AiB}(X,Z)$, and it is given by

$$\mathrm{AiB}(X,Z) = e^{i(XZ-2Z^3/3)}\mathrm{Ai}(X-Z^2), \tag{2}$$

where $Z \equiv z\kappa^2/2k$ is the (scaled) dimensionless propagation distance with wavenumber k. Figure 1(e) shows $|\mathrm{AiB}(X,Z)|^2$, where the transverse acceleration is apparent since the beam follows the parabola $X = Z^2$, which is plotted as a solid white line. The fringes of $\mathrm{AiB}(X,Z)$ extend indefinitely for the infinite-energy case, suggesting that an arbitrarily large transverse acceleration is possible with increasing Z. This is a direct consequence of the infinite power of the initial function.

To make its energy finite, the Airy function's spectrum can be sharply truncated [8–10]. Since the Airy beam is defined as a Fourier integral over its entire spectrum, a sharp cutoff gives the incomplete Airy function [13,14]

$$\mathrm{Ai}^{\mathrm{inc}}_{M,W}(X) \equiv \frac{1}{2\pi}\int_{M-W}^{M+W} \mathrm{d}\xi \, \exp\left[i\left(\frac{1}{3}\xi^3 + \xi X\right)\right], \tag{3}$$

where M is the center of the integration window and W determines its width. This function is similar to Eq. (1)

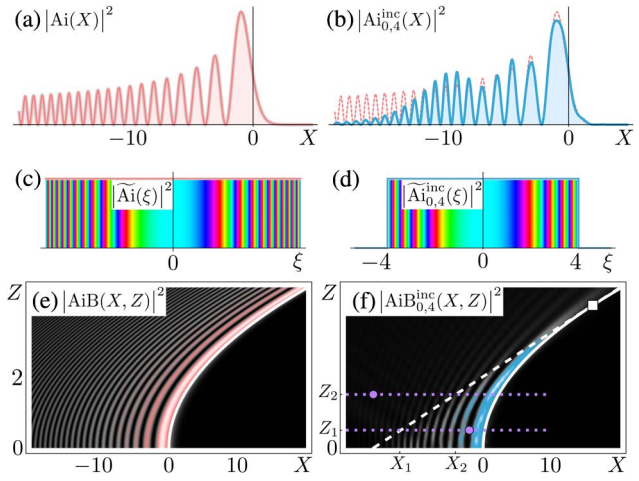

Fig. 1. Comparison of infinite and incomplete Airy beams with $M = 0$, $W = 4$. (a) $|\mathrm{Ai}(X)|^2$, (b) $|\mathrm{Ai}^{\mathrm{inc}}_{0,4}(X)|^2$ in blue, $|\mathrm{Ai}(X)|^2$ in dotted pink, (c) $|\widetilde{\mathrm{Ai}}(\xi)|^2$, shading by hue indicates the phase, (d) $|\widetilde{\mathrm{Ai}}^{\mathrm{inc}}_{0,4}(\xi)|^2$, (e) $|\mathrm{AiB}(X,Z)|^2$, and (f) $|\mathrm{AiB}^{\mathrm{inc}}_{0,4}(X,Z)|^2$, symmetric about $Z = 0$; white dashed line shows Eq. (8), which meets the solid white parabola $X = Z^2$ at Eq. (9) (white square); purple dots correspond to the complex planes of Figs. 2(a) and 2(b); dotted lines at Z_1 and Z_2 indicate slices plotted in Figs. 2(c) and 2(d); Eq. (5) is like Airy right of the white dashed line.

but with a finite domain of integration, and is incomplete since only part of the spectrum is included.

Figure 1(c) shows $|\widetilde{\mathrm{Ai}}(\xi)|^2$, which is nonzero for all ξ. Figure 1(d) shows $|\widetilde{\mathrm{Ai}}^{\mathrm{inc}}_{0,4}(\xi)|^2$ which agrees with $\widetilde{\mathrm{Ai}}(\xi)$ in the range $-4 < \xi < 4$ and is zero otherwise. Figure 1(b) shows the intensity of Eq. (3) as a shaded blue line for $M = 0$ and $W = 4$, compared with that of $\mathrm{Ai}(X)$. A visible consequence of the sharp cutoff is a small oscillating modulation of the Airy fringes before they die away. This can result in a main lobe with increased intensity as observed in [8,9]. The subsequent total intensity is given elegantly by Parseval's theorem as

$$\int_{-\infty}^{\infty} \mathrm{d}X |\mathrm{Ai}^{\mathrm{inc}}_{M,W}(X)|^2 = W/\pi. \tag{4}$$

The simplicity of this exact result motivates our subsequent analytic investigation. We call the paraxially propagating form of Eq. (3) the incomplete Airy beam, $\mathrm{AiB}^{\mathrm{inc}}_{M,W}(X,Z)$, and it is given by

$$\mathrm{AiB}^{\mathrm{inc}}_{M,W}(X,Z) = e^{i(XZ-2Z^3/3)}\mathrm{Ai}^{\mathrm{inc}}_{M-Z,W}(X-Z^2). \tag{5}$$

The intensity of Eq. (5) is plotted in Fig. 1(f). The expectation value of the transverse position of the beam is given by Ehrenfest's theorem as

$$\bar{X} = -W^2/3 - M^2 + 2MZ, \tag{6}$$

which is linear in Z. This demonstrates that, despite the appearance of acceleration in Eq. (5), the beam's center only moves linearly proportional to MZ.

A remarkable property of Eq. (5) is that the integration limits of $\mathrm{Ai}^{\mathrm{inc}}_{M-Z,W}(X-Z^2)$ change as $M - Z \pm W$, continuously translating in the direction of negative ξ. This is a consequence of shifting the integration variable after propagation to recover an Airy-like function with no ξ^2 term. The significance of this shift becomes apparent through a saddle point approximation of Eq. (5). Since the exponent of Eq. (5) is cubic, in the oscillatory region ($Z^2 > X$) it is necessary to sum contributions from two saddles at

$$\xi_\pm = \pm\sqrt{Z^2 - X}. \tag{7}$$

Importantly though, Airy-like oscillations only occur when the finite integration contour crosses both saddles. As Z increases, the endpoints move to exclude the saddles from the integral and the oscillations decay as the intensity becomes increasingly dependent on contributions to the integral from near the endpoints instead of from Airy-like interference of two saddles.

A complex plane representation of the exponent in the integral of Eq. (5) is shown in Fig. 2(a), which corresponds to an Airy-like region of the beam since both saddles are included on the integration contour between the endpoints. As Z increases, the endpoints move in the direction indicated by the white arrows. When the upper endpoint crosses over the saddle, the contribution from ξ_+ is excluded since it is no longer on the integration contour, and the function stops being Airy-like. Figure 2(b) shows the complex plane in this case.

We note that the dashed white lines in Figs. 2(a) and 2(b) are not the paths of steepest descent, but the usual arguments still apply since approximation of the exact path must still exclude saddles outside the endpoints.

It is then possible to determine explicitly the region where the beam has Airy-like behavior, since the line where the endpoint crosses the upper saddle can be found by equating Eq. (7) to $\mu_\pm - Z$, where $\mu_\pm = M \pm W$ is the original cutoff. Therefore, the beam stops being Airy-like outside the region bounded by the lines

$$X_\pm = 2Z\mu_\pm - \mu_\pm^2. \tag{8}$$

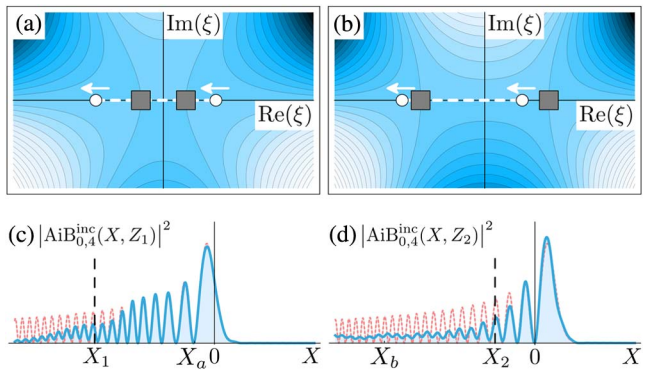

Fig. 2. (a), (b) Complex planes with real contours of $i\xi^3/3 + i\xi(X_{a,b} - Z^2_{1,2})$, respectively, corresponding to lower and upper purple dots of Fig. 1(f). Gray squares are saddles of Eq. (7), white dots are endpoints, white dashed line shows the integration contour. (a) Airy-like configuration and (b) non-Airy-like configuration. (c), (d) Show intensity along dashed purple lines of Fig. 1(f) at Z_1 and Z_2, respectively, the vertical black, dashed lines show intercepts $X_{1,2}$ of the line of Eq. (8) with $Z_{1,2}$.

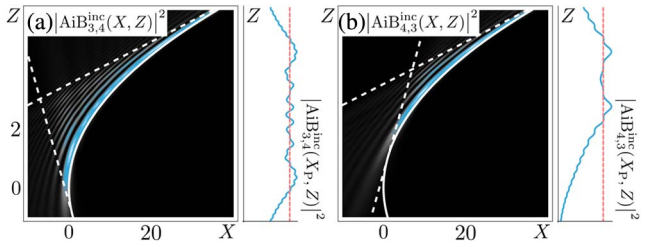

Fig. 3. $|\mathrm{AiB}^{\mathrm{inc}}_{M,W}(X,Z)|^2$ for $M \neq 0$; dashed lines are given by Eq. (8) and enclose the Airy-like region of the beam. (a) $M = 3$ and $W = 4$ with enhanced main lobe and (b) $M = 4$ and $W = 3$. Side plots show main lobe intensity against that of (dashed) $\mathrm{AiB}(X_\mathrm{P}, Z)$; X_P is the X coordinate of the ideal beam's peak intensity.

The white dashed line in Fig. 1(f) is Eq. (8) for μ_+. $\mathrm{AiB}^{\mathrm{inc}}_{0,4}(X,Z)$ is Airy-like only to the right of this line, while to the left its oscillations decay in both amplitude and spacial frequency, far more rapidly than a standard Airy pattern. Figures 2(c) and 2(d) show slices of intensity along the purple dashed lines of Fig. 1(f) at distances Z_1 and Z_2. The vertical dashed lines at X_1 and X_2 correspond to Eq. (8) for Z_1 and Z_2, respectively, and they therefore mark the transition between Airy-like and not.

The incomplete Airy beam also provides an explicit expression for the maximum extent of the main lobe, which follows the same path as for the infinite-energy beam, but decays as it approaches the line of Eq. (8). Therefore, the main lobe propagates no further than

$$(X,Z) = (\mu_+^2, \mu_+), \tag{9}$$

which is shown as a white square in Fig. 1(f). After this point the main lobe's intensity rapidly decays since the saddles are excluded from the integral of Eq. (5). Accordingly, the lobe forms after the point (μ_-^2, μ_-).

In the region of the main lobe, and away from the lines of Eq. (8), the incomplete Airy beam can be approximated by the infinite-energy Airy beam, $\mathrm{AiB}(X,Z)$, plus a first-order endpoint-correction term, $E_{M,W}(X,Z)$. In the simplest case of $M = 0$, this correction term is

$$E_{0,W}(X,Z) = e^{-iW^2 Z} \sin\left[WX + \frac{1}{3}W^3\right]/\pi W^2, \tag{10}$$

which describes the additional oscillating modulation visible in Fig. 1(b) and is valid for asymptotically large W. The correction is more complicated for $M \neq 0$, but is not difficult to calculate via endpoint asymptotics.

Choosing $M \neq 0$ for the incomplete Airy function selects a different portion of the spectrum to generate the incomplete Airy beam. It is therefore possible to prescribe what region of the beam is Airy-like, since the endpoints will enclose the saddles in different places. Figure 3(a) shows the incomplete Airy beam for an initial spectral truncation of $-1 \leq \xi \leq 5$, and Fig. 3(b) shows the case for $1 \leq \xi \leq 7$. The dashed lines are given by Eq. (8) and correspond to the intersections of endpoints with saddles. The dynamics of both ξ_+ and ξ_- are important. Airy oscillations occur only within the enclosed regions and the beam is no longer symmetric about $Z = 0$. We note that the dashed lines are always tangential to the curve $X = Z^2$, and so can also be thought of as the extremal rays of a fold caustic [16].

It is then possible to optimize the extent of the main lobe for fixed W at the cost of symmetry about $Z = 0$. Figure 3(a) shows an enhanced main lobe (produced at the expense of secondary fringes) for the same W as Fig. 1(f), but now with $M = 3$. Of course, the resolution of a generating SLM might still impose some limitations.

In previous studies, an Airy beam's spectrum has been manipulated to control the ballistic regime [11] and secondary lobe intensity [10]. Our analytic results here complement these by providing, for the incomplete Airy beam, explicit expressions for the spatial extent of the Airy-like behavior of the beam in terms of the cutoff parameter, including the maximum extent of the main lobe. Initial investigation indicates they also loosely approximate the dynamics of less severe cutoffs.

References

1. J. Durnin, J. Opt. Soc. Am. A **4**, 651 (1987).
2. M. V. Berry and N. L. Balazs, Am. J. Phys. **47**, 264 (1979).
3. J. D. Ring, J. Lindberg, A. Mourka, M. Mazilu, K. Dholakia, and M. R. Dennis, Opt. Express **20**, 18955 (2012).
4. J. Durnin, J. J. Miceli, Jr., and J. H. Eberly, Phys. Rev. Lett. **58**, 1499 (1987).
5. G. A. Siviloglou and D. N. Christodoulides, Opt. Lett. **32**, 979 (2007).
6. M. A. Bandres and J. C. Gutiérrez-Vega, Opt. Express **15**, 16719 (2007).
7. M. Zamboni-Rached, K. Z. Nóbrega, and C. A. Dartora, Opt. Express **20**, 19972 (2012).
8. L. Carretero, P. Acebal, S. Blaya, C. Garcia, A. Fimia, R. Madrigal, and A. Murciano, Opt. Express **17**, 22432 (2009).
9. M. I. Carvalho and M. Facão, Opt. Express **18**, 21938 (2010).
10. S. Barwick, Opt. Lett. **36**, 2827 (2011).
11. Y. Hu, P. Zhang, C. Lou, S. Huang, J. Xu, and Z. Chen, Opt. Lett. **35**, 2260 (2010).
12. D. M. Cottrell, J. A. Davis, and T. M. Hazard, Opt. Lett. **34**, 2634 (2009).
13. L. Levey and L. B. Felsen, Radio Sci. **4**, 959 (1969).
14. J. D. Ring, J. Lindberg, C. J. Howls, and M. R. Dennis, J. Opt. **14**, 075702 (2012).
15. M. V. Berry and C. J. Howls, "Integrals with coalescing saddles," http://dlmf.nist.gov/36.2.
16. M. V. Berry and C. Upstill, Prog. Opt. **18**, 257 (1980).